PREPARATION AND STRUCTURAL CHARACTERIZATION OF RAPIDLY SOLIDIFIED Al-Si ALLOYS

B. VARGA[1]   E. FAZAKAS[2]   L.K. VARGA[3]

Abstract: *Rapidly solidified hypereutectic Al_{100-x}-Si_x alloys (x = 12; 20; 40 wt.%) with cost effective minor additions (Ni, Ti, Fe and P) have been prepared and analysed. The increased cooling rate and the minor additives determine an expansion of the coupled growth area, which is displayed asymmetrically in relation to the eutectic point, thus favouring the formation of nano and amorphous structures. Fe and P additives are structure refiners leading to nano-sized Al and Si grains and the Ni and Ti additives result in a homogeneous amorphous as cast structure.*

Key words: *silumin, rapidly solidified, primary silicon.*

1. Introduction

Al-Si alloys have a number of remarkable technological and operational properties: excellent castability, particularly of silumins of eutectic composition, good machinability, good corrosion resistance and wear resistance properties. At the same time, the increase in the silicon contents determines the diminishing of the thermal dilatation coefficient in these alloys, which reaches values close to the ones specific for cast iron (at approximately 40 wt.% Silicon), Figure 1. We have to point out that the classical processing technology of these alloys by casting only use hypoeutectic and eutectic compositions. Improving the technological and operational properties of these compositions requires finishing the primary silicon and the eutectic separations. It is well known that grain size distribution and morphologies of primary silicon in hypereutectic silumins play an important role in determining their mechanical properties. The coarse separations of primary silicon have an unfavourable effect both on machinability and processing properties. Conventional ingot metallurgy yields a polygonal, star-shaped and coarse plated primary silicon phase that limits the further improvement of the properties of hypereutectic Al-Si alloys. The reduction in size of primary silicon separations can be achieved metallurgically, by introducing new elements, as well as by intensifying the cooling rate.

The paper studies the cumulated influence of the cooling rate and of the various additives on the dispersity and size of the phases in hypereutectic silumins. At the same time, the research aimed at identifying the conditions determining a nano or even amorphous structure of hypereutectic silumins.

---

[1] Dept. of Technologic Equipment and Materials Science, *Transilvania* University of Braşov.
[2] Institute for Materials Science and Technology (BAY-ATI), Budapest, Hungary.
[3] Research Institute for Solid State Physics and Optics of Hungarian Acad. of Science, Budapest, Hungary.
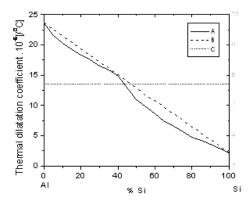
Fig. 1. *Variation of the thermal dilatation coefficient in the Al-Si system compared to the motor cylinder:*
A. measured values: for chill-cast silumins (0…40% Si);
processed by atomisation pressing (50…100% Si) [1]
B. theoretical values, computed by the law of additivity;
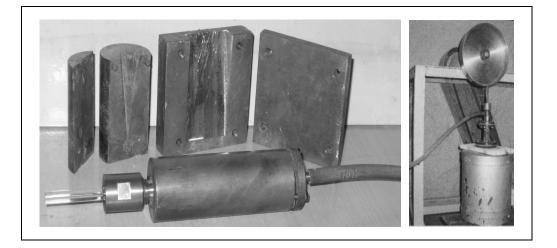*C. for the cylinder material (cast iron)*

Fig. 2. *Devices for the high cooling rate processing of aluminium based alloys:*
a) wedge sample chill; b) pyramid sample chill; c) suction based chill and
d) device for producing thin ribbons with ultra-rapid cooling [9]

2. Applied Rapid Solidification Techniques

In (moulding) sand casting the usual cooling rate is of 10^0 °C/s, while in chill casting it reaches 10^2 °C/s. Several techniques were used for the processing of samples solidified at high cooling rates:

a) casting of wedge (key) and pyramid type samples in copper chills, Figures 2a and 2b;

b) suction casting in graphite mould placed in copper mould supports, Figures 2c and 3;

c) solidification of the liquid jet on the

exterior surface of the spinning disk (melt spinning). The liquid is ejected onto the rotating drum in two variants, bottom-up and up-down. The installation for the bottom-up variant was home made at *Transilvania* University of Braşov, Figure 2d.

The evaluation of the cooling rate [4], is based on the equation (1):

$$d = A \cdot v^{-n}, \tag{1}$$

where: d - is the distance between the secondary dendrite arms or the diameter of the primary silicon separations, in µm; v - the cooling rate, in °C/s; A, n - constants.

Fig. 3. *Laboratory vacuum sucking device*

Two compositions were used for which equation (1) is known [7], [8] for a large solidification rate interval, (see Table 1 and Figure 4).

By determining the dimensions of the primary phases in samples processed under different conditions, and by applying equation (1) with the constants from Table 1, the cooling rates achievable by the presented devices could be calculated. The estimated values of the cooling rates for the 4 devices are presented in Table 2.
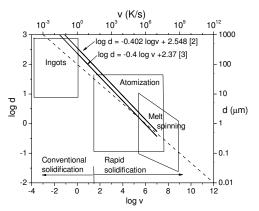

Fig. 4. *Interdependence: Cooling rate vs. Dendrite parameters* [6-8]

3. Experimental Procedure

Experimental determinations were carried out in parallel at *Transilvania* University of Braşov and at the Institute for Solid State Physics and Optics, Budapest.

At the University of Braşov, samples were processed by means of the devices presented in Table 2. Within the experimental determinations, the basic material used for the three compositions was a hypereutectic industrial alloy [%]: Si - 23.97; Mg - 0.06; Mn - 0.04; Fe - 0.7; Cu - 0.21; Cr - 0.012; Zn - 0.1; Ni - 0.08; Ti - 0.05; Pb - 0.026; Sn - 0.003. The adjustment of the compositions for the three alloys was achieved by alloying with aluminium and silicon, respectively.

Titanium and phosphor were used for finishing the structure. Titanium and nickel were used in order to obtain nano and amorphous structures [2], [5]. It needs to be pointed out that while the Al-Si and Al-Ni systems include eutectic, the Al-Ti system includes peritectic.

The three compositions were smelted at the Institute for Solid State Physics and Optics of Budapest. In this case only high

Values of constants A and n   Table 1

Composition	Phase	n	log [A]	References
Al-Si 18%	Primary Silicon	0.402	2.548	[8]
Al-Si 7%	Solid solution α	0.4	2.37	[7]

Estimated values of the cooling rates by device type   Table 2

Device Code	Device type, product dimensions [mm] (length x thickness/thickness)	Cooling rate [ºC/s]
a	Wedge sample chill 50 x 10	10^2 - 5×10^2
b	Pyramid sample chill 50 x (10-10-10)	5×10^2 - 10^3
c	Suction chill 100 x 1.0; x 0.7; x Φ1	5×10^3 - 10^4
d	Spinning disk ribbon 0.030…0.100	5×10^5 - 5×10^6

Table 3

Experimental conditions for high cooling rate solidification of Al-Si alloys

Sample code	Spinning disk		Speed		Jet extrusion technology	Alloy					
	Material	Diameter [cm]	Speed [rot/min]	Peripheral velocity [m/s]		Al-Si12*	Al-Si20*		Al-Si40*		
						$Al_{88}Si_{12}$**	$Al_{80}Si_{20}$**	$Al_{79}Si_{11}Ni_{10-x}Ti_x$** x=0…10	$Al_{60}Si_{40}$**	$Al_{55}Si_{37}Fe_6P_2$**	$Al_{51}Si_{30}Fe_6P_2Ni_9Ti_2$**
1Bv	steel	20	3150	33	from below		●				
2Bv			1800	19			●				
3Bp	copper	15	4200	33	from above, in Ar atmosphere	●	●	●	●	●	●
4Bp			3400	27		●	●				
5Bp			2600	20		●	●				

Note: *composition expressed in wt. %; **composition expressed in molar fractions.

purity primary metals were used and processed by the up-down melt spinning method. This casting was carried out in argon atmosphere.

Table 3 shows a synthesis of the completed experiments.

4. Structure and Properties of the Processed Compositions

The processed compositions were qualified following the structure analysis by means of the optic microscope, SEM and X rays, further by thermal analysis and dilatometry.

Due to the high cooling rate, the structure of the ribbon samples of Al-Si12 composition consists only of solid α solution. This observation is confirmed by the X ray image of Figure 5.

Hence, due to the high cooling rate silicon solubility in the solid α solution has increased from 1.6 wt.% (equilibrium concentration) to 12 wt.%.

During tempering operations, silicon

precipitates are formed at temperatures exceeding 320…360 °C. On the dilatometric curve, this process is marked by an inflexion point.
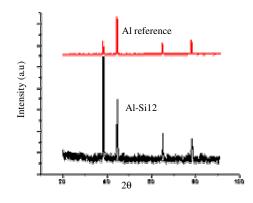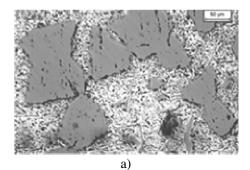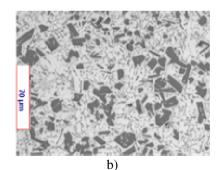

Fig. 5. *X ray diffractograms for the Al-Si12 composition*

In the case of the $Al_{80}Si_{20}$ composition, the structural modifications determined by the increase in cooling rate are presented in the micrographs of Figure 6.

Based on the analysis of the presented microstructures, it can be noticed that an increased cooling rate also yields qualitative modifications in addition to the finishing of the structure, involving the occurrence of the hypoeutectic structure in a hypereutectic composition. This observation is in accordance with the data from literature concerning the extension of the coupled growth area under the influence of high cooling rates and its asymmetrical display in relation to the concentration of the eutectic point [3]. At the same time, the obtained structural modifications are more
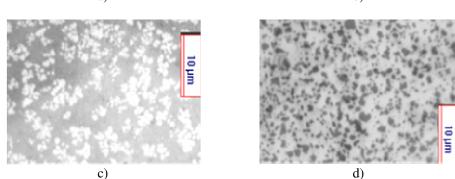

a)

b)

c)

d)

Fig. 6. *Quantitative and qualitative modifications determined by the increase in the cooling rate, in the case of a hypereutectic silumin $Al_{80}Si_{20}$:*
a) sand casting; b) wedge sample chill casting; c) melt-spinning casting;
d) structure of sample c after tempering at 400 ºC

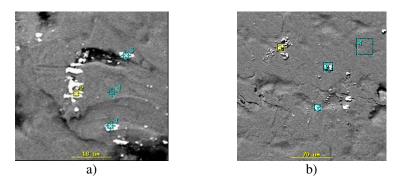<div style="text-align:center">a)　　　　　　　　　　b)</div>

Fig. 7. *Defect points on the smooth surface of Al-Si20 ribbons, with increased concentrations of alloying elements in points 1, 2 and 3: a) iron and b) zinc*

intensive than those mentioned in literature for a similar composition [10].

It needs to be mentioned that the smooth surfaces of the ribbons processed by the two spinning disk variants (steel-feed from below and copper-feed from above) are comparable as to their quality. In the case of samples 1Bv and 2Bv, SEM analyses have highlighted that increased local concentrations of iron (61…67%) and zinc (22…26%) correspond to the defect points on the smooth surface of the ribbons, Figure 7.

The tendency of nano and amorphous structure forming in the quaternary Al-Si-Ni-Ti system was studied by the processing of $Al_{79}Si_{11}Ni_{10-x}Ti_x$ ($x = 0…10$) compositions, obtained by replacing the silicon in the Al-Si20 basic composition by (Ni+Ti).
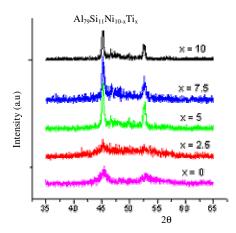

Fig. 8. *X ray diffractograms recorded for $Al_{79}Si_{11}Ni_{10-x}Ti_x$ ($x = 0…10$) compositions*

The obtained X ray images are presented in Figure 8. The amorphous structure of composition $Al_{79}Si_{11}Ni_{10-x}Ti_x$ ($x = 2.5$) was confirmed also by thermal analysis (DSC).

Figure 9 shows the X ray images for compositions based on the Al-Si40 alloy. For the rapidly solidified $Al_{60}Si_{40}$ system, silicon precipitates of 0.5…1.5 microns were obtained. Doping with Fe-P refines the structure without introducing further

intermetallic compound phases. Based on Scherrer's formula, the grain size for Al is 53 nm and for Si 63 nm. Further doping with Ti and Ni changes the phase composition, the Al nanograins disappear as well as the 60 nm Si grains.

Subsequent heat treatment of the nanostructured ribbon samples revealed their excellent stability up to 450 °C. Thus, after tempering of the $Al_{55}Si_{37}Fe_6P_2$ ribbon at 450 °C for 70 hours, the structure remained submicroscopic.
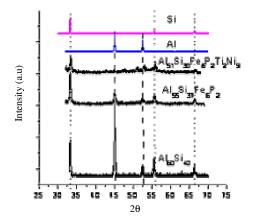

Fig. 9. *X ray diffractograms recorded for compositions based on the Al-Si40 system*

The dilatometric analysis of the $Al_{60}Si_{40}$ composition performed on test pieces taken from the centre of the chill cast sample (Table 2, variant a) highlighted that the value of the thermal dilatation coefficient varies significantly with temperature. At temperatures in the 100-300 °C range the value of the thermal dilatation coefficient is of $12 \cdot 10^{-6}$, and for high temperatures of 450-550 °C, the coefficient is $6 \cdot 10^{-6}$.

5. Conclusions

The increased cooling rate and/or minor additives determines an extension of the coupled growth area, displayed asymmetrically in relation to the eutectic point, thus favouring the generation of nano and amorphous structures within the Al-Si system.

Experimental determinations have shown the possibility of obtaining the nano and amorphous structures in typical industrial alloys (Al-Si) by doping with cost effective

and available elements (Ni, Ti and P).

The additions, for which the coupled growth area is displayed asymmetrically in relation to the eutectic concentration, favor the formation of the amorphous structure (see, for example, the Al-Ni system).

Measurements have confirmed the small values of the thermal dilatation coefficient in the case of silumins with high silicon concentrations.

Acknowledgments

References

1. David, M.J.: *Spray Formed Silicon-Aluminium.* In: Advanced Materials & Processes (2000) No. 3, p. 36.
2. Dermarker, S.: *Amorphous Al-Based Alloys Essentially Containing Ni*

and/or Fe and Si and Process for the Production Thereof. United States Patent, Number 4.731.133, data Mar. 15/1988.

3. Genau, A.L.: *Microstructural Development in Al-Si Powder during Rapid Solidification.* Iowa State University, Ames, 2004.

4. Granger, D.A.: *Ingot Casting in the Aluminium Industry.* In: Treatise on Materials Science and Technology, Ed. A.K. Vasudevan, R.D. Doherty **31** (1989), p. 109.

5. Kawazoe, Y., Masumoto, T., Suzuki, K., Inoue, A., Tsai, P.A., Yu, Z.J., Aihara, T. jr., Nakanomyo, T.: *Phase Diagrams and Physical Properties of Nonequilibrium Alloys. Subvolume A: Nonequilibrium Phase Diagrams of Ternary Amorphous Alloys.* Springer, 1996.

6. Kear, Bh.: *Rapid Solidification Technology.* In: Journal of Metals **34** (1982) No. 8, p. 36; *Cutting Edge Technologies.* Washington. The National Academy Press, 1984.

7. Shivkumar, S., Wang, L., Apelian, D.**:** *Molten Metal Processing of Advanced Cast Aluminium Alloys.* In: JOM (1991) No. 2, p. 26.

8. Şmakov Iu, V., Zenina, M.V., Riabov, I.V.: *Sovremennoje sostoianie i dalnejichee razvitie porchnevah splavov na Al-osnove.* In: Liteinoe Proizvodstvo (2000) No. 11, p. 3.

9. Varga, B.: *Procedure and Installation for Manufacturing Ultra-Rapidly Cooled Metal Ribbons.* In: Metalurgia **58** (2006) No. 6, p. 5.

10. Xu, L.C., Wang, Y.H., Qiu, F., Yang, F.Y, Jiang, Q.C.: *Cooling Rate and Microstructure of Rapidly Solidified Al-20 wt.% Si Alloy.* In: Materials Science and Engineering A, **417** (2006), p. 275.